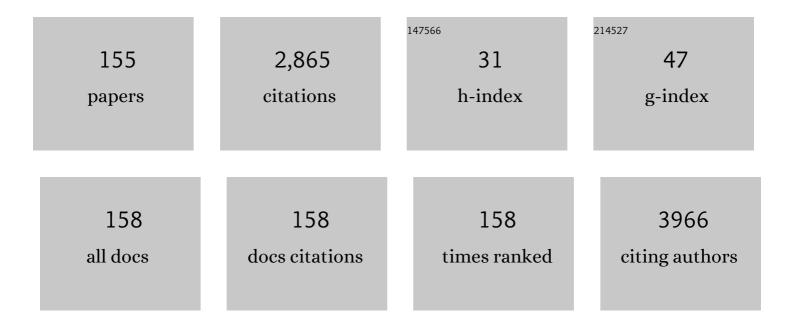
## Hyung-Kook Kim

List of Publications by Year in descending order

Source: https://exaly.com/author-pdf/9562699/publications.pdf Version: 2024-02-01



HYUNG-KOOK KIM

#	Article	IF	CITATIONS
1	The growth mechanism and optical properties of ultralong ZnO nanorod arrays with a high aspect ratio by a preheating hydrothermal method. Nanotechnology, 2009, 20, 155603.	1.3	161
2	Solution-derived 40 µm vertically aligned ZnO nanowire arrays as photoelectrodes in dye-sensitized solar cells. Nanotechnology, 2010, 21, 195602.	1.3	134
3	Bioinspired piezoelectric nanogenerators based on vertically aligned phage nanopillars. Energy and Environmental Science, 2015, 8, 3198-3203.	15.6	115
4	Photoluminescence of polycrystalline ZnO under different annealing conditions. Journal of Applied Physics, 2003, 94, 5787-5790.	1.1	90
5	Enhanced Sunlight Harvesting of Dye-Sensitized Solar Cells Assisted with Long Persistent Phosphor Materials. Journal of Physical Chemistry C, 2013, 117, 17894-17900.	1.5	83
6	Aerodynamic and aeroelastic flutters driven triboelectric nanogenerators for harvesting broadband airflow energy. Nano Energy, 2017, 33, 476-484.	8.2	81
7	A study on the Raman spectra of Al-doped and Ga-doped ZnO ceramics. Current Applied Physics, 2009, 9, 651-657.	1.1	73
8	Freestanding ZnO nanorod/graphene/ZnO nanorod epitaxial double heterostructure for improved piezoelectric nanogenerators. Nano Energy, 2015, 12, 268-277.	8.2	72
9	Color-tunable properties of Eu3+- and Dy3+-codoped Y2O3 phosphor particles. Nanoscale Research Letters, 2012, 7, 556.	3.1	61
10	Preparation and electrochemical characterization of porous SWNT–PPy nanocomposite sheets for supercapacitor applications. Synthetic Metals, 2008, 158, 638-641.	2.1	53
11	Study of Nitrogen Adsorbed on Single-Walled Carbon Nanotube Bundles. Journal of Physical Chemistry B, 2002, 106, 3371-3374.	1.2	50
12	A facile route to aligned TiO2 nanotube arrays on transparent conducting oxide substrates for dye-sensitized solar cells. Journal of Materials Chemistry, 2011, 21, 5062.	6.7	47
13	Strain effects in ZnO thin films and nanoparticles. Journal of Applied Physics, 2006, 99, 064308.	1.1	46
14	The glass transition temperatures of sugar mixtures. Carbohydrate Research, 2006, 341, 2516-2520.	1.1	45
15	Cu-doped flower-like hematite nanostructures for efficient water splitting applications. Journal of Physics and Chemistry of Solids, 2016, 98, 283-289.	1.9	45
16	Versatile nanodot-patterned Gore-Tex fabric for multiple energy harvesting in wearable and aerodynamic nanogenerators. Nano Energy, 2018, 54, 209-217.	8.2	45
17	Mesoporous silica with fibrous morphology: a multifunctional core–shell platform for biomedical applications. Nanotechnology, 2013, 24, 345603.	1.3	43
18	Study of Nitrogen Adsorbed on Open-Ended Nanotube Bundles. Journal of Physical Chemistry B, 2003, 107, 1540-1542.	1.2	42

#	Article	IF	CITATIONS
19	Binding of caffeine with caffeic acid and chlorogenic acid using fluorescence quenching, UV/vis and FTIR spectroscopic techniques. Luminescence, 2016, 31, 565-572.	1.5	42
20	Study of the structural evolution in ZnO thin film by in situ synchrotron x-ray scattering. Journal of Applied Physics, 2004, 96, 1740-1742.	1.1	40
21	Advantages of using Ti-mesh type electrodes for flexible dye-sensitized solar cells. Nanotechnology, 2012, 23, 225602.	1.3	38
22	Tailoring the luminescent properties of Gd2O3:Tb3+ phosphor particles by codoping with Al3+ ions. Journal of Alloys and Compounds, 2012, 541, 263-268.	2.8	38
23	Growth and properties of Li2B4O7 single crystals doped with Cu, Mn and Mg. Journal of Crystal Growth, 2003, 249, 483-486.	0.7	37
24	Facile synthesis of bifunctional silica-coated core–shell Y2O3:Eu3+,Co2+ composite particles for biomedical applications. RSC Advances, 2012, 2, 9495.	1.7	37
25	Inhibitory effect of traditional oriental medicine-derived monoamine oxidase B inhibitor on radioresistance of non-small cell lung cancer. Scientific Reports, 2016, 6, 21986.	1.6	37
26	Impurity band characteristics near the band edge of Al-doped ZnO. Journal of Applied Physics, 2004, 96, 1507-1510.	1.1	35
27	Quantum confinement in Volmer–Weber-type self-assembled ZnO nanocrystals. Applied Physics Letters, 2005, 86, 193113.	1.5	35
28	Bifunctional Gd2O3:Er3+ particles with enhanced visible upconversion luminescence. Journal of Alloys and Compounds, 2013, 572, 113-117.	2.8	34
29	Synthesis and Characterization of Flower-Like Bundles of ZnO Nanosheets by a Surfactant-Free Hydrothermal Process. Journal of Nanomaterials, 2014, 2014, 1-11.	1.5	34
30	Pt-coated TiO 2 nanorods for photoelectrochemical water splitting applications. Results in Physics, 2016, 6, 373-376.	2.0	34
31	Ultrafine PEG-capped gadolinia nanoparticles: cytotoxicity and potential biomedical applications for MRI and luminescent imaging. RSC Advances, 2014, 4, 34343-34349.	1.7	31
32	Synthesis and luminescence properties of Ho3+ doped Y2O3 submicron particles. Journal of Physics and Chemistry of Solids, 2012, 73, 176-181.	1.9	30
33	Submicron Y2O3 particles codoped with Eu and Tb ions: Size controlled synthesis and tuning the luminescence emission. Journal of Colloid and Interface Science, 2012, 373, 14-19.	5.0	30
34	Effects of solvent polarity on the absorption and fluorescence spectra of chlorogenic acid and caffeic acid compounds: determination of the dipole moments. Luminescence, 2016, 31, 118-126.	1.5	30
35	Synthesis and optical properties of Dy3+-doped Y2O3 nanoparticles. Journal of the Korean Physical Society, 2012, 60, 244-248.	0.3	29
36	Ti-doped hematite thin films for efficient water splitting. Applied Physics A: Materials Science and Processing, 2015, 118, 1539-1542.	1.1	28

#	Article	IF	CITATIONS
37	Eu, Gd-Codoped Yttria Nanoprobes for Optical and T1-Weighted Magnetic Resonance Imaging. Nanomaterials, 2017, 7, 35.	1.9	28
38	Dye-sensitized solar cells composed of photoactive composite photoelectrodes with enhanced solar energy conversion efficiency. Journal of Materials Chemistry A, 2015, 3, 11130-11136.	5.2	27
39	Water-Through Triboelectric Nanogenerator Based on Ti-Mesh for Harvesting Liquid Flow. Journal of the Korean Physical Society, 2018, 72, 499-503.	0.3	27
40	A flexible lead-free piezoelectric nanogenerator based on vertically aligned BaTiO3 nanotube arrays on a Ti-mesh substrate. RSC Advances, 2016, 6, 81426-81435.	1.7	26
41	Multicolor nanoprobes based on silica-coated gadolinium oxide nanoparticles with highly reduced toxicity. RSC Advances, 2016, 6, 19758-19762.	1.7	26
42	TiO2 nanofiber/nanoparticles composite photoelectrodes with improved light harvesting ability for dye-sensitized solar cells. Electrochimica Acta, 2016, 193, 166-171.	2.6	26
43	Study of Argon Adsorbed on Open-Ended Carbon Nanotube Bundles. Journal of Physical Chemistry B, 2002, 106, 9000-9003.	1.2	25
44	Efficient and hysteresis-less perovskite and organic solar cells by employing donor-acceptor type Ĩ€-conjugated polymer. Organic Electronics, 2019, 72, 18-24.	1.4	25
45	The liquid–glass transition in sugars: Relaxation dynamics in trehalose. Journal of Non-Crystalline Solids, 2006, 352, 4464-4474.	1.5	24
46	The optical properties of Eu3+ and Tm3+ codoped Y2O3 submicron particles. Journal of Alloys and Compounds, 2012, 525, 8-13.	2.8	24
47	Fabrication of bifunctional core-shell Fe3O4 particles coated with ultrathin phosphor layer. Nanoscale Research Letters, 2013, 8, 357.	3.1	24
48	Structural relation and epitaxial properties of hexagonal InN and oxidized cubic In2O3. Solid State Communications, 2004, 130, 397-400.	0.9	23
49	Making monosaccharide and disaccharide sugar glasses by using microwave oven. Journal of Non-Crystalline Solids, 2004, 333, 111-114.	1.5	23
50	Luminescent core–shell Fe3O4@Gd2O3:Er3+, Li+ composite particles with enhanced optical properties. Journal of Sol-Gel Science and Technology, 2014, 71, 391-395.	1.1	22
51	Near-edge x-ray absorption fine structure and x-ray photoemission spectroscopy study of the InN epilayers on sapphire (0001) substrate. Journal of Applied Physics, 2004, 95, 5540-5544.	1.1	19
52	Synchrotron x-ray scattering study on the evolution of surface morphology of the InN/Al2O3(0001) system. Applied Physics Letters, 2002, 81, 475-477.	1.5	18
53	Nanogenerators facilitated piezoelectric and flexoelectric characterizations for bioinspired energy harvesting materials. Nano Energy, 2021, 81, 105607.	8.2	18
54	Scalable and inexpensive strategy to fabricate CuO/ZnO nanowire heterojunction for efficient photoinduced water splitting. Journal of Materials Science, 2018, 53, 2725-2734.	1.7	17

#	Article	IF	CITATIONS
55	Electrical properties of Li2B4O7 single crystals in the [001] direction: Comparison between crystals grown from Li2CO3 and B2O3 mixed powder and from Li2B4O7 powder. Journal of Applied Physics, 2002, 92, 4644-4648.	1.1	16
56	Study of alkyl chain length dependent characteristics of imidazolium based ionic liquids [CnMIM]+[TFSA]â^' by Brillouin and dielectric loss spectroscopy. Current Applied Physics, 2013, 13, 271-279.	1.1	16
57	Dual-mode spectral convertors as a simple approach for the enhancement of hematite's solar water splitting efficiency. Applied Physics A: Materials Science and Processing, 2015, 119, 1373-1377.	1.1	16
58	Effects of Oxygen Pressure on the Crystalline of ZnO Films Grown on Sapphire by PLD Method. Journal of the Korean Physical Society, 2005, 47, 300.	0.3	16
59	Jamming transition in a highly dense granular system under vertical vibration. Physical Review E, 2005, 72, 011302.	0.8	15
60	Fabrication of carbon coated gadolinia particles for dual-mode magnetic resonance and fluorescence imaging. Journal of Advanced Ceramics, 2015, 4, 118-122.	8.9	15
61	Highly sensitive detection of epidermal growth factor receptor expression levels using a capacitance sensor. Sensors and Actuators B: Chemical, 2015, 209, 438-443.	4.0	15
62	Synchrotron x-ray scattering study of lattice relaxation in InN epitaxial layers on sapphire(0001) during dc sputter growth. Journal of Applied Physics, 2002, 92, 5814-5818.	1.1	14
63	Probing the interaction of caffeic acid with ZnO nanoparticles. Luminescence, 2016, 31, 654-659.	1.5	13
64	Morphological and structural characterization of epitaxial α-Fe2O3 (0001) deposited on Al2O3 (0001) by dc sputter deposition. Journal of Vacuum Science and Technology A: Vacuum, Surfaces and Films, 2005, 23, 1450-1455.	0.9	12
65	Oxidation study of polycrystalline InN film using in situ X-ray scattering and X-ray photoemission spectroscopy. Thin Solid Films, 2007, 515, 4691-4695.	0.8	12
66	Controlled growth of ZnO nanorod templates and TiO2 nanotube arrays by using porous TiO2 film as mask. Journal of Sol-Gel Science and Technology, 2008, 47, 187-193.	1.1	12
67	Synthesis and Photoluminescence Properties of Ho <sup>3+</sup> Doped LaAlO3 Nanoparticles. Journal of Nanoscience and Nanotechnology, 2012, 12, 5847-5851.	0.9	12
68	Cytotoxicity and cell imaging potentials of submicron colorâ€ŧunable yttria particles. Journal of Biomedical Materials Research - Part A, 2012, 100A, 2287-2294.	2.1	12
69	Effect of the dielectric layer on the electrical output of a ZnO nanosheet-based nanogenerator. Journal of the Korean Physical Society, 2015, 67, 1920-1924.	0.3	12
70	The secondary relaxation in the dielectric loss of glucose–water mixtures. Journal of Non-Crystalline Solids, 2006, 352, 4679-4684.	1.5	11
71	Covalent attachment of polystyrene on multi-walled carbon nanotubes via nitroxide mediated polymerization. Composite Interfaces, 2007, 14, 493-504.	1.3	11
72	Morphology transformation from ZnO nanorod arrays to ZnO dense film induced by KCl in aqueous solution. Thin Solid Films, 2008, 517, 626-630.	0.8	11

#	Article	IF	CITATIONS
73	Critical Thickness of AlN Thin Film Grown on Al2O3(0001). Japanese Journal of Applied Physics, 2001, 40, 4677-4679.	0.8	10
74	Dielectric properties of Li3VO4 single crystals grown by the Czochralski method. Journal of Applied Physics, 2003, 93, 1697-1700.	1.1	10
75	ac conductance of surface layer in lithium tetraborate single crystals. Journal of Applied Physics, 2003, 94, 7246-7249.	1.1	10
76	Study of dielectric relaxations of anhydrous trehalose and maltose glasses. Journal of Chemical Physics, 2011, 134, 014508.	1.2	10
77	Discrimination of Defective (Full Black, Full Sour and Immature) and Nondefective Coffee Beans by Their Physical Properties. Journal of Food Process Engineering, 2014, 37, 524-532.	1.5	10
78	Facile Covalent Attachment of Well-Defined Poly( <i>t</i> -butyl acrylate) on Carbon Nanotubes via Radical Addition Reaction. Journal of Nanoscience and Nanotechnology, 2008, 8, 4598-4602.	0.9	9
79	Synthesis and optical properties of Gd2O3:Pr3+ phosphor particles. Journal of Sol-Gel Science and Technology, 2012, 64, 156-161.	1.1	9
80	Highly Durable Ti-Mesh Based Triboelectric Nanogenerator for Self-Powered Device Applications. Journal of Nanoscience and Nanotechnology, 2016, 16, 4864-4869.	0.9	9
81	New 2D-Conjugated Polymer for Non-Halogenated and Halogenated Solvents Processed Organic Solar Cells. Macromolecular Research, 2018, 26, 1276-1279.	1.0	9
82	Raman Study of the Effects of Hydrogen Gas Annealing on PbTiO3Crystals. Japanese Journal of Applied Physics, 2003, 42, 1292-1296.	0.8	8
83	Effects of Al–Mn coâ€doping on magnetic properties of semiconducting oxide thin films. Physica Status Solidi (B): Basic Research, 2014, 251, 2274-2278.	0.7	8
84	Oxidation study of InN/sapphire (0001) film usingin-situ synchrotron X-ray scattering. Physica Status Solidi A, 2004, 201, 2777-2781.	1.7	7
85	TiO <sub>2</sub> Thin Films Sensitized with Upconversion Phosphor for Efficient Solar Water Splitting. Journal of Nanoscience and Nanotechnology, 2017, 17, 7647-7650.	0.9	7
86	Covalent attachment of poly(ethylene glycol) on multi-walled carbon nanotubes. Composite Interfaces, 2006, 13, 321-328.	1.3	6
87	Temperature dependent vibrational modes of glycosidic bond in disaccharide sugars. Carbohydrate Research, 2008, 343, 660-667.	1.1	6
88	Preparation and characterization of nanostructured composite films for organic light emitting diodes. Journal of Physics: Conference Series, 2009, 187, 012029.	0.3	6
89	A study of dielectric relaxations in galactose–water mixtures. Journal of Non-Crystalline Solids, 2010, 356, 2836-2841.	1.5	6
90	Improved conversion efficiency of dye-sensitized solar cell based on the porous anodic TiO2 nanotubes. Current Applied Physics, 2011, 11, S320-S323.	1.1	6

#	Article	IF	CITATIONS
91	Effects of Li <sup>+</sup> Codoping on the Optical Properties of SrAl <sub><b>2</b></sub> O <sub><b>4</b></sub> Long Afterglow Ceramic Phosphors. Advances in Optics, 2014, 2014, 1-4.	0.3	6
92	WO3–ZnO and CuO–ZnO nanocomposites as highly efficient photoanodes under visible light illumination. Nanotechnology, 2020, 31, 255702.	1.3	6
93	Study of the Strain in InN Thin Films Using Synchrotron X-Ray Scattering. Japanese Journal of Applied Physics, 2002, 41, 1932-1935.	0.8	5
94	Growth of high-quality βII-Li3VO4 single crystals by the Czochralski method. Journal of Crystal Growth, 2003, 259, 115-120.	0.7	5
95	Identification of hexagonal polycrystal in epitaxially grown InN by synchrotron x-ray diffraction and near-edge x-ray absorption fine structure spectroscopy. Applied Physics Letters, 2003, 82, 2981-2983.	1.5	5
96	Growth of Na modified potassium lithium niobate crystal by the Czochralski method. Journal of Crystal Growth, 2004, 270, 370-375.	0.7	5
97	The structural and optical properties of Volmer–Weberâ€ŧype ZnO nanorods. Physica Status Solidi (A) Applications and Materials Science, 2011, 208, 1021-1026.	0.8	5
98	Ratiometric pH Sensor Based on Fluorescent Core–Shell Nanoparticles. Journal of Nanoscience and Nanotechnology, 2017, 17, 8313-8316.	0.9	5
99	Characterization of performance parameters of organic solar cells with a buffer ZnO layer. Advances in Natural Sciences: Nanoscience and Nanotechnology, 2019, 10, 015005.	0.7	5
100	The Liquid Glass Transition in Sugars and Sugar Mixtures. AIP Conference Proceedings, 2006, , .	0.3	4
101	Enhanced Stokes and Anti-Stokes Photoluminescence Emission from LaAIO <sub>3</sub> :Nd <sup>+3</sup> Nanosized Powder Coated with a SiO <sub>2</sub> Shell Layer. Journal of Nanoscience and Nanotechnology, 2011, 11, 5892-5897.	0.9	4
102	Compressed-exponential relaxations in supercooled liquid trehalose. Current Applied Physics, 2012, 12, 1548-1552.	1.1	4
103	Energy harvesting of dye-sensitized solar cells assisted with Ti-mesh and phosphor materials. IOP Conference Series: Materials Science and Engineering, 2014, 54, 012025.	0.3	4
104	Exploring the use of impedance spectroscopy in relaxation and electrochemical studies. Applied Spectroscopy Reviews, 2018, 53, 157-176.	3.4	4
105	A Comparative Study of the Effects of Different Methods for Preparing RGO/Metal-Oxide Nanocomposite Electrodes on Supercapacitor Performance. Journal of the Korean Physical Society, 2020, 76, 264-272.	0.3	4
106	Solubility of V2O5 in Polycrystalline ZnO with Different Sintering Conditions. Journal of the Korean Physical Society, 2005, 47, 333.	0.3	4
107	Effect of Annealing Ti Foil on The Structural Properties of Anodic TiO2 Nanotube Arrays. Journal of the Korean Physical Society, 2011, 58, 575-579.	0.3	4
108	Study on the phases of RVO <sub>4</sub> (R=Dy, Eu, Gd, Yb) ceramics. Ferroelectrics, 1990, 109, 191-195.	0.3	3

#	Article	IF	CITATIONS
109	Study on the phase transitions in Bi <sub>(1 - x)</sub> Gd <sub>x</sub> VO <sub>4</sub> ceramics I. Ferroelectrics, 1990, 109, 197-202.	0.3	3
110	Critical thickness and surface oxidation of epitaxial AIN thin films. Integrated Ferroelectrics, 1999, 24, 129-137.	0.3	3
111	Dielectric Non-Linearity in the Tetragonal Direction of Li2B4O7 Single Crystals. Journal of the Physical Society of Japan, 2001, 70, 3119-3123.	0.7	3
112	Synchrotron x-ray scattering study of SnO <sub>2</sub> thin film grown on sapphire. Journal of Materials Research, 2002, 17, 2417-2422.	1.2	3
113	Effects of the Nano-Tubular Anodic TiO <sub>2</sub> Buffer Layer on Bioactive Hydroxyapatite Coating. Journal of Nanoscience and Nanotechnology, 2011, 11, 286-290.	0.9	3
114	Single-Crystalline Twinned ZnO Nanoleaf Structure via a Facile Hydrothermal Process. Journal of Nanoscience and Nanotechnology, 2011, 11, 2175-2184.	0.9	3
115	Investigation of ultraviolet carrier recombination of Volmer-Weber type ZnO nanocrystals and nanorods through Varshni's formula and Arrhenius plots. Journal of the Korean Physical Society, 2012, 60, 466-471.	0.3	3
116	Effect of Er3+ and Yb3+ co-doping on the performance of a ZnO-based DSSC. Journal of the Korean Physical Society, 2016, 68, 1381-1389.	0.3	3
117	Preparation of ZnO Nanorod/Graphene/ZnO Nanorod Epitaxial Double Heterostructure for Piezoelectrical Nanogenerator by Using Preheating Hydrothermal. Journal of Visualized Experiments, 2016, , e53491.	0.2	3
118	Spectroscopic study of binding of chlorogenic acid with the surface of ZnO nanoparticles. Russian Journal of Physical Chemistry A, 2017, 91, 1781-1790.	0.1	3
119	Controlled in situ capacitance sensing of single cell via simultaneous optical tweezing. Sensors and Actuators B: Chemical, 2020, 321, 128512.	4.0	3
120	A Study of Structures in ZnO and ZnO:V2O5 Thin Films by In-Situ Synchrotron X-ray Scattering. Journal of the Korean Physical Society, 2007, 51, 862.	0.3	3
121	Study on the phases in Bi <sub>(1 - x)</sub> Gd <sub>x</sub> VO <sub>4</sub> ceramics II. Ferroelectrics, 1990, 109, 185-190.	0.3	2
122	Ferroelectric and Electric Properties of the PZT/ZnO Hybrid Thin Films. Ferroelectrics, 2002, 268, 11-16.	0.3	2
123	Fabrication of Volmer-Weber Type ZnO Nanorods by Combining RF Sputtering and Hydrothermal Methods. Journal of Nanoscience and Nanotechnology, 2009, 9, 6993-7.	0.9	2
124	Effects of N- and N-In doping on ZnO films prepared by using ultrasonic spray pyrolysis. Journal of the Korean Physical Society, 2014, 65, 1890-1895.	0.3	2
125	Synthesis and physical properties of zinc-oxide textured films by using a filtered preheated hydrothermal. Journal of the Korean Physical Society, 2014, 65, 1423-1429.	0.3	2
126	Heat Generation by Ion Friction in Water under an AC Electric Field. Journal of the Korean Physical Society, 2019, 75, 832-840.	0.3	2

#	Article	IF	CITATIONS
127	Growth Dynamics and Size Distribution of Self-Assembled ZnO Nanocrystals on a Metal Pt(111) Substrate. Journal of the Korean Physical Society, 2007, 51, 887.	0.3	2
128	Synthesis of Carbon Nanotube-CuxO(x=8, 64) Nanocrystal Composites. Journal of the Korean Physical Society, 2010, 56, 421-424.	0.3	2
129	Transient Behavior of DC and AC Conductance in Li2B4O7 Single Crystals. Journal of the Korean Physical Society, 2005, 47, 317.	0.3	2
130	Characterization of Buried Ultrathin Layer and Multilayer System by X-Ray Scattering. Japanese Journal of Applied Physics, 2002, 41, 3039-3042.	0.8	1
131	Rapid Estimation of the Height-Height Correlation Functions from the Synchrotron X-Ray and AFM Study of very Thin SnO2/α-Al2O3(0001) FILM. International Journal of Modern Physics B, 2003, 17, 1183-1187.	1.0	1
132	Nano-Particle Size Measurement by Photon Correlation Spectroscopy and Dielectric Loss Spectroscopy. AIP Conference Proceedings, 2006, , .	0.3	1
133	A Study of the Secondary Relaxation in Galactose-Water Mixtures. AIP Conference Proceedings, 2008, ,	0.3	1
134	Characterizations of Sodium Modified Potassium Lithium Niobate Crystal. Ferroelectrics, 2009, 382, 7-15.	0.3	1
135	The Fabrication of TiO2 Mesoporous Thick Films by Employing a Pre-Embedded ZnO Nanorods Support. Journal of Nanoscience and Nanotechnology, 2009, 9, 7145-9.	0.9	1
136	Optical and Electrical Properties of Ultralong ZnO Nanorod Fabricated from Preheating Hydrothermal Method. Journal of Nanoscience and Nanotechnology, 2011, 11, 463-469.	0.9	1
137	Unusual Melting Transition of Nitrogen Physisorbed on Carbon Nanotube Bundles. Journal of Nanoscience and Nanotechnology, 2011, 11, 6580-6583.	0.9	1
138	Annealing Effects of Sapphire Substrate on the Structure and Properties of ZnO Films Grown via Pulsed Laser Deposition. Journal of Nanoscience and Nanotechnology, 2011, 11, 584-588.	0.9	1
139	Effect of nanoscale confinement on dielectric relaxations in a 3wt.% water-galactose mixture. Journal of the Korean Physical Society, 2012, 60, 1092-1096.	0.3	1
140	Cell-based capacitance sensor for analysis of EGFR expression on cell membrane. , 2013, , .		1
141	Relaxation processes in disaccharide sugar glasses. , 2013, , .		1
142	Structural and Electronic Characteristics of ZnO Thin Films dc Sputtered on Sapphire (0001) Substrates. Journal of the Korean Physical Society, 2008, 52, 1685-1688.	0.3	1
143	Quick Phase Search Method on an Adsorbed System. Journal of the Korean Physical Society, 2007, 50, 1281.	0.3	1
144	Effect of Nano-scale Confinement on Dielectric Relaxation in a 3 wt.% Water-Galactose Mixture. New Physics: Sae Mulli, 2011, 61, 406-412.	0.0	1

#	Article	IF	CITATIONS
145	Infrared reflection studies of γâ€ray irradiated NaNO2. Journal of Applied Physics, 1981, 52, 2808-2811.	1.1	0
146	A two-inch dc/rf circular magnetron sputtering gun for a miniature chamber for an in situ experiment. Review of Scientific Instruments, 1998, 69, 1616-1621.	0.6	0
147	Study of dielectric relaxations in glucose-water mixtures. AIP Conference Proceedings, 2004, , .	0.3	0
148	Low Frequency Impedance Study of Li2B4O7Single Crystals. Ferroelectrics, 2005, 326, 109-112.	0.3	0
149	Dehydration Processes of Sugar Glasses and Crystals. AIP Conference Proceedings, 2006, , .	0.3	0
150	Effects of Disaccharide Sugars on Dynamics of Water Molecules: Dynamic Light Scattering and Dielectric Loss Spectroscopy Studies. AlP Conference Proceedings, 2008, , .	0.3	0
151	Effects of the disaccharide concentration and the extrusion speed on the size of unilamella vesicles. Current Applied Physics, 2011, 11, 1401-1404.	1.1	0
152	A Study of the Structure in a ZnO/MgO Multilayer by Using a Synchrotron X-ray Scattering Method. Journal of the Korean Physical Society, 2007, 51, 866.	0.3	0
153	Influence of the Interface Property on the Memory Function in a CER Cell Based on Pr0.7Ca0.3MnO3 Films. Journal of the Korean Physical Society, 2007, 51, 545-549.	0.3	0
154	The Cooperation Effect of Mixed PEGs with Different Molecular Weights on The Morphology of TiO2 Porous Thin Films. Journal of the Korean Physical Society, 2010, 56, 413-416.	0.3	0
155	Improvement of Electrodeposition Rate of Cu Layer by Heat Treatment of Electroless Cu Seed Layer. Korean Journal of Materials Research, 2014, 24, 186-193.	0.1	Ο